JGeope 3 (1), 2013, P. 69-78

Chemical characteristics of biotite from Boroujerd Granitoid complex (Middle Jurassic), Western Iran

Dariush Esmaeily [1], Reza Maghdour-Mashhour [1]*, Amir Ali Tabbakh Shabani [2]
[1] *Department of Geology, University College of Sciences, University of Tehran, Tehran, Iran*
[2] *Faculty of Earth Sciences, Kharazmi University, Tehran, Iran*
**Corresponding author, e-mail: samer.mashour@gmail.com*

(*received: 21/09/2012 ; accepted: 29/05/2013*)

Abstract

Biotite samples from different units of Boroujerd Granitoid Complex (BGC) of the Sanandaj-Sirjan Zone, western Iran, have been analyzed by electron microprobe for major elements. Biotite analyses from three units of quartzdiorite, granodiorite and monzogranite of BGC have their own distinct non-overlapping compositional fields in the annite – siderophyllite – phlogopite – eastonite quadrilateral (ASPE), reflecting their host rock compositions. Biotite from each rock unit has an increasing trend of Al contents at almost fixed Fe/(Fe+Mg) values. In quartzdiorite it shows an approximately constant range of Fe/(Fe+Mg) with a low to moderate Al content from 2.5 to 3 atoms per formula unit (apfu). Biotite from granodiorite exhibits a fairly wide range of Al values reaching up to 3.32 apfu, at Fe/(Fe+Mg) from 0.6 to 0.7, whereas biotite from monzogranite have a relatively narrow range of Fe/(Fe+Mg) and total Al values of limited range of 3.1 to 3.3 apfu. Biotite compositions from these two latter units considered to be derived entirely from crustal material, characterized by a remarkable increase in total Al at relatively high Fe contents. Biotite samples of quartzdiorites define a distinct and non-overlapping trend from those of granidiorites and monzogranites and hence interpreted to be derived from a parental magma with different composition. Calculation of log(XMg/XFe) ranges from -0.09 to -0.02 and most of samples from quartzdiorite fall within weakly and moderately contaminated I-type field of log(XF/XOH) versus log(XMg/XFe) diagram, whereas the other two units, containing biotites with log(XMg/ XFe)< -0.21, classified as strongly contaminated reduced I-type. Oxygen fugacity (log $fO2$) of -15.4 to -17.5 bars and $fH2O$ of 200 to 560 bars were calculated for quartzdiorite. Likewise, log (fO_2) of –17.66 bars and water fugacity (fH_2O) of 400 and 700 bars were also calculated for granodiorite and monzogranites respectively. In the FeO*–MgO–Al_2O_3 biotite discrimination diagram, biotite compositions from BGC are distributed between the calc-alkaline and peraluminous fields, i.e., biotite from the qaurtzdioritic rocks fall principally in the calc-alkaline field, whereas those from the granodioritic and monzogranitic units plot almost exclusively in the peraluminous field consistent with their host rock nature.

Keywords: *Biotite, Chemical composition, Petrogenesis, Oxygen fugacity, Granitoid, Sanandaj-Sirjan zone, Iran*

Introduction

Biotite, a ubiquitous ferromagnesian mineral of granitoids, proved to be a valuable guide to their petrogenesis (Ague & Brimhall, 1988; Shabani *et al.,* 2003). Its composition is classically used to estimate the physico-chemical conditions of crystallization of the parental magma such as chemical composition, oxygen and halogen fugacities (Speer, 1984) and even to evaluate the tectono-magmatic environment of its host-rock (e.g., Wones & Eugster, 1965; Nachit *et al.,* 1985; Patino-Douce, 1993; Patino-Douce *et al.,* 1993; Lalonde & Bernard, 1993; Burkhard, 1991, 1993; Abdel-Rahman, 1994; El Sheshtawi *et al.,* 1993; Hecht 1994; Stone *et al.,* 1997; Stone, 2000; Li *et al.,* 2003; Aydin *et al.,* 2003; Buda *et al.,* 2004; Bónová *et al.,* 2010; Shabani *et al.,* 2010).

Most recent detailed geological, geochemical and petrological studies, carried out on Boroujerd granitoid complex (BGC) by Ahmadi-Khalaji *et al.,* (2007) indicate that the complex belongs to metaluminous to slightly peraluminous, high K calc-alkaline series and displays geochemical characteristics of I-type volcanic arc granites related to an active continental margin. Further investigations on biotite composition by Moazami Goudarzi, (2006) and Ahmadi-khalaji, (2009) corroborate these findings as well.

Having proposed by the above mentioned researchers, the potential of biotite as a reliable petrogenetic and tectonomagmatic indicator of its host; also bridging the gaps and reducing probable uncertainties in the evaluation and interpretation of earlier thesis or papers, chemistry of biotite, as a dominant mafic mineral in nearly all types of BGC, has been used in this study to better constrain our understanding regarding the nature of host granitic magma, petrogenesis and geodynamics of the BGC. In this study, we documented by electron microprobe the chemical composition of 57 points on biotites from 6 rock samples taken from different units of BGC. Of these specimens, 3 samples were analyzed by wet chemistry to document the oxidation state of iron. In addition, the results of 35 point analyses of biotite taken from the literature have been included in our data set (Moazami Goudarzi, 2006; Ahmadi-khalaji *et al.,* 2009).

Geological setting

The BGC is the largest of several plutonic bodies within the 1500 km-long, NW-SE trending Sanandaj-Sirjan zone (SSZ) in western Iran (Fig. 1), a complex structural zone comprising metamorphosed and multiply-deformed volcanic rocks, metasediments, ophiolite sequences and granitoid plutons of mostly Mesozoic ages. The occurrence of SSZ is generally interpreted in terms of the opening and closure of the Late Permian – Miocene Neo-Tethyan Ocean. The timing for the opening of the Neo-Tethyan Ocean is well constrained some time during the Sakmarian to Late Wordian interval (Stampfly & Borel, 2002), whereas closure had been at Miocene epoch (e.g. Berberian *et al.,* 1982; Sengor *et al.,* 1988; Sengor & Natalin, 1996). The BGC comprises three main units: quartz diorite, granodiorite and monzogranite whereby the granodiorite is the dominant one (Fig. 1). Zircon U-Pb ages for these three plutonic units overlap, with a total spread from 169.6±0.2 to 173.7±1.5 Ma (Ahmadi-Khalaji *et al.,* 2007; Mahmoudi *et al.,* 2011).

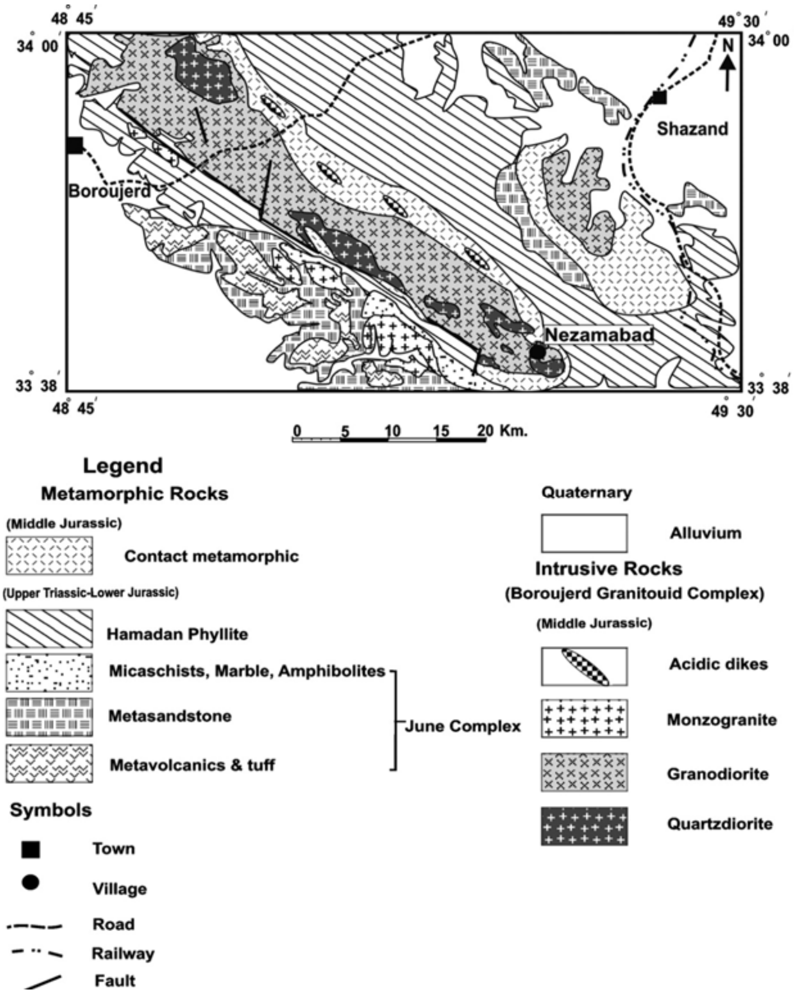

Figure 1: A simplified geological map of Boroujerd granitoid complex (after Ahmadi-Khalaji *et al.,* 2007).

Material and Methods:

Analytical Methods:

Electron Microprobe Analysis

Biotite analyses were obtained on polished thin sections prepared from each rock sample described above for 12 elements using a Cameca SX-50 electron microprobe at the Universite´ Paul-Sabatier, Toulouse, France. Typical beam operating conditions were 15 kV and probe current 15 nA. The counting time for analysis of each element was 20 seconds except for F, 30 seconds. The accuracy of the analyses is 1% for major and 10% for minor elements. The standards used for the elemental analyses were as follow: synthetic fluorphlogopite for F, wollastonite for Si and Ca, corundum for Al, magnetite for Fe, periclase for Mg, rutile for Ti, sylvite for Cl, barite for Ba, pure Mn for Mn, orthoclase for K and jadeite for Na. Finally, matrix effects were corrected using the PAP Program provided by Pouchou and Pichoir (1984, 1985). A total of 59 point analyses were collected. Average chemical composition of studied samples with their respective structural formulae based on 24(O, OH, F, Cl) anions are presented in Table (2).

Table 1: Chemical composition of the investigated granitoids. Oxides in wt. %, trace elements in ppm (data from Ahmadi-Khalaji *et al.,* 2007).

Granitoid	*Quartzdiorite*		*Granodiorite*			*Monzogranit*
Samples	**G12**	**B2A3**	**G5**	**C11**	**AD4**	**B3A9**
SiO_2 (%)	56.3	58.9	63.4	64.9	59.7	69.7
Al_2O_3	17.1	16.2	16.1	16	20.2	14.9
Fe_2O_3	8.0	7.1	5.2	4.5	4.3	2.5
MgO	5.1	4.7	1.5	1.4	1.3	0.5
CaO	6.9	5.9	3.8	2.5	5.2	1.8
Na_2O	2.5	2.5	2.9	3.1	3.6	4.1
K_2O	2.1	2	3.4	4	3.4	4.2
TiO_2	0.9	0.7	0.6	0.5	0.6	0.2
P_2O_5	0.2	0.1	0.1	0.1	0.2	0
MnO	0.2	0.1	0.1	0.1	0	0.1
LOI	0.6	1.5	2.2	2.5	1.5	1.5
Total	99.9	99.7	99.3	99.6	100	99.7
Ni (ppm)	75	49	19	18	10	8
Cr	360	320	90	150	100	110
Co	27.8	23.8	11.1	10.2	8.9	3.5
V	204	150	81	60	50	11
Cs	5.4	4.7	3	9.3	4.3	4.5
Rb	88.2	77.4	122	146	133.	152.5
Sr	347	231	295	256	484	132.5
Ba	355	361	551	577	1150	372
Th	9	5	17	21	14	13
U	2.4	2.3	2.5	1.9	2.3	2.6
Ta	0.9	0.9	0.9	1	0.8	.1
Nb	12	10	14	14	15	11
Hf	5	4	6	5	9	5
Zr	161.	123.5	198.	179.	341	149
Zn	127	58	51	43	53	47
Ga	22	18	21	21	25	17
Sn	3	2	1	2	2	4
W	8	14	4	15	5	11
La	27.2	16.4	40.7	47.3	64	25.1
Ce	57.6	41.5	82.5	91.1	118.	54.5
Pr	6.7	5.7	8.6	9.6	11.6	5.6
Nd	25	24	30	32.3	38.8	20.3
Sm	5	5.4	5.2	5.3	6.2	4.4
Eu	0.4	0.8	0.9	1.2	2.2	0.2
Gd	5.1	5.3	4.7	6	6.3	4.2
Tb	0.7	0.8	0.6	0.7	0.8	0.6
Dy	4.3	5.1	3.6	3.8	3.6	4.1
Ho	0.8	1.0	0.7	0.7	0.5	0.8
Er	2.6	3.2	2	2	1.2	2.7
Tm	0.4	0.5	0.3	0.2	0.1	0.4
Yb	2.5	3.2	1.8	1.7	0.8	2.6
Lu	0.4	0.5	0.3	0.2	0.1	0.4
Y	23.4	30.2	19.6	19.2	15	23.3
A/CNK	0.9	0.9	1.04	1.14	1.06	1.02

FeO and Fe_2O_3 Determination

Contents of FeO and Fe_2O_3 were determined for three different samples of biotite separates from every unit through wet chemistry in the chemistry laboratory of the Geological Survey of Iran. To separate mica from rock for ferrous and ferric iron determination, whole rock samples were crushed using both jaw crusher and pulverizer. The crushed samples were then sieved to obtain the size fraction between 45 and 60 mesh (350-250 μm). All samples were washed with water to remove dust. Magnetite was removed with a strong permanent magnet and the mafic and felsic grains were then separated using heavy liquids (methylene iodide, S.G. = 3.33). Final shaking on a tilted paper sheet and hand-picking were performed for all samples until the biotite concentrates appeared at least 99% pure under the binocular microscope. Then to prevent contamination and oxidation of ferrous iron, the biotite grains were ground under acetone in an agate mortar and pestle to obtain a fine powdered sample. Powdered mica dissolves more readily during acid attack than the granular micas and thus yields higher precision and accuracy of ferrous and ferric iron determinations.

Petrographical and geochemical characteristics:

Granodiorite, the relatively dominant unit of BGC, forms a large elongated NW-extending pluton (Fig. 1). It has the approximate modal composition of 30– 40% plagioclase which forms zoned euhedral to subhedral laths, 10–20% biotite, 25–30% quartz and <20% alkali feldspar. It shows clear foliation due to the orientation of minerals. Apatite, zircon, allanite, chlorite, titanite, prehnite and opaques are accessory minerals. Muscovite is present as a secondary mineral.

The monzogranitic unit is widely scattered as separate and small outcrops through the southern part of the area (Fig. 1). Mineral assemblages include quartz (30–35%), perthitic alkali feldspar (30–35%), zoned plagioclase (25–35%), biotite (5–10%) and some secondary muscovite. Zircon, allanite and apatite are common accessory minerals.

Zoned euhedral to subhedral megacrysts of plagioclase (40–50%), biotite (15–20%), green amphibole (10–15%), quartz (<15%) and alkali feldspar (<5%) are the dominant modal composition of quartzdioritic unit. Chlorite, epidote, prehnite, zircon, titanite and apatite are accessory minerals.

Biotite generally occurs as subhedral sporadically euhedral dark brown kinked flakes that vary from 1 to 3 mm in diameter in all units of BGC. It commonly encloses scattered primary accessories such as apatite, zircon and sometimes alanite. The presence of numerous minute inclusions of primary accessories trapped during biotite growth, suggests, along with biotite interstitial grain position, its primary magmatic origin.

Major and trace elements of the investigated granitoids (Table 1) show metaluminous to slightly peraluminous nature, typical of I type granites. It belongs to high-K calc-alkaline series and displays the geochemical characteristics typical of volcanic arc granites related to an active continental margin (e.g. significant Nb, Ti, P and Sr depletion). Isotopic data (Sr_i = 0.7062–0.7074 and $_{\varepsilon}Ndt$ = -3.02 to -3.62) are consistent with a crustal protolith (Ahmadi-Khalaji *et al.,* 2007). Trends of the major elements also suggest that the granodiorite and monzogranite may be co-magmatic and quartzdiorite has been interpreted to be derived from parental magma with different composition or distinct process (Ahmadi-Khalaji *et al.,* 2007).

Mineral chemistry

The 57 points from 6 samples, analyzed from rocks of the BGC, are all trioctahedral common micas (5 < *M* site < 6 atoms per formula unit, apfu) and, for the different units fall within biotite field. Average biotite compositions and their calculated structural formulae based on 24(O,OH,F,Cl) are presented in Table 2.

The major element chemistry of the micas shows average TiO_2 contents in all samples from 1.84 to 3.20 wt%. It changes from 2.2 to 3.5 wt% in qaurtzdiorite, 1.5 to 2.9 in granodiorite and 2 to 2.5 for monzogranite unit. Consequently Ti cations vary between (0.14 - 0.41), (0.6 – 0.38) and (0.22 – 0.33) apfu in these units respectively.

As shown by Lalonde and Bernard (1993) and Shabani *et al.,* (2003) biotite is perhaps the most common mineralogical sink for excess aluminum in granitic rocks. The peraluminosity index (A/CNK) of whole-rock samples (Table 1) ranging from 0.9 to 1.1 whereas of biotites (Table 2) varies approximately between 1.4 and 1.7, indicating clearly biotite higher A/CNK values relative to those of its host rock.

Table 2: Electron microprobe analyses of biotite from BGC along with their respective structural formulae calculated based on 24(O,OH,F,Cl).

Granitoids	***Quartzdiorite***				***Granodiorite***					***Monzogranite***		
Ref.	**This study**		**Ahmadi, (2009)**	**Moazami , (2006)**	**This study**			**Ahmadi, (2009)**	**Moazami, (2006)**	**This study**	**Ahmadi, (2009)**	**Moazami , (2006)**
Samples No. of analyses	**G12 (n=7)**	**B2A31 (n=4)**	**(n=6)**	**(n=15)**	**G5 (n=12)**	**C11 (n=13)**	**AD4 (n=10)**	**(n=3)**	**(n=6)**	**B3A9 (n=11)**	**(n=3)**	**(n=2)**
SiO_2	36.43	36.37	36.66	35.01	34.85	34.45	34.31	34.19	33.25	34.38	33.90	35.24
TiO_2	3.20	2.41	3.51	2.45	2.42	1.84	2.41	1.89	2.43	2.29	1.96	3.22
Al_2O_3	14.69	16.44	15.09	15.11	16.63	17.74	17.35	18.57	17.97	17.28	18.10	18.02
FeO	15.28	15.13	15.03	16.46	19.44	19.05	20.43	18.88	20.86	22.04	20.03	20.79
Fe_2O_3	3.48	3.44	3.81	3.17	3.81	3.73	4.01	4.63	3.84	3.33	4.91	3.25
MgO	11.41	11.35	11.73	12.01	7.27	7.83	6.59	7.62	7.04	5.44	5.94	4.63
CaO	0.04	0.02	0.03	0.23	0.09	0.04	0.02	0.06	0.19	0.01	0.03	0.09
Na_2O	0.07	0.06	0.15	0.10	0.06	0.08	0.04	0.17	0.10	0.03	0.05	0.14
K_2O	9.18	9.34	8.53	10.64	9.25	9.21	9.16	8.05	10.51	9.27	8.32	10.96
BaO	0.27	0.12	0.00	0.00	0.20	0.19	0.23	0.00	0.00	0.13	0.00	0.00
F	0.31	0.39	0.00	0.41	0.39	0.30	0.76	0.00	0.45	0.55	0.00	0.37
Cl	0.49	0.27	0.00	0.19	0.31	0.45	0.36	0.00	0.20	0.17	0.00	0.14
H_2O(c)	3.68	3.65	4.00	3.98	3.50	3.55	3.33	4.00	3.94	3.45	4.00	3.89
O=F	0.13	0.16	0.00	0.17	0.16	0.13	0.32	0.00	0.19	0.23	0.00	0.16
O=Cl	0.11	0.06	0.00	0.04	0.07	0.10	0.08	0.00	0.05	0.04	0.00	0.03
Sum Ox%	98.29	98.75	98.53	99.54	98.00	98.23	98.60	98.06	100.54	98.11	97.24	100.52
Mineral formulae based on 24(O,OH,F,Cl)												
Si	5.57	5.52	5.55	5.35	5.46	5.37	5.37	5.29	5.13	5.43	5.33	5.41
ΣAl(afpu)	2.65	2.94	2.69	2.72	3.07	3.26	3.20	3.39	3.27	3.22	3.36	3.26
Al/Al^{IV}	2.43	2.48	2.45	2.65	2.54	2.63	2.63	2.71	2.87	2.57	2.67	2.59
ΣT	8.00	8.00	8.00	8.00	8.00	8.00	8.00	8.00	8.00	8.00	8.00	8.00
Al^{VI}	0.22	0.46	0.24	0.07	0.54	0.63	0.57	0.68	0.41	0.65	0.69	0.68
Ti	0.37	0.28	0.40	0.28	0.29	0.22	0.28	0.22	0.28	0.27	0.23	0.37
Fe^{2+}	1.95	1.92	1.90	2.11	2.55	2.48	2.67	2.44	2.69	2.91	2.63	2.67
Fe^{3+}	0.40	0.39	0.43	0.36	0.45	0.44	0.47	0.54	0.45	0.40	0.58	0.38
Mg	2.60	2.57	2.64	2.74	1.70	1.82	1.54	1.76	1.62	1.28	1.39	1.06
ΣM	5.54	5.61	5.62	5.56	5.52	5.59	5.54	5.63	5.45	5.52	5.52	5.16
Ca	0.01	0.00	0.00	0.04	0.01	0.01	0.00	0.01	0.03	0.00	0.01	0.01
Na	0.02	0.02	0.04	0.03	0.02	0.02	0.01	0.05	0.03	0.01	0.02	0.04
K	1.79	1.81	1.65	2.08	1.85	1.83	1.83	1.59	2.07	1.87	1.67	2.15
Ba	0.02	0.01	0.00	0.00	0.01	0.01	0.01	0.00	0.00	0.01	0.00	0.00
ΣI	1.84	1.84	1.70	2.14	1.90	1.88	1.86	1.65	2.13	1.89	1.69	2.20
F	0.15	0.19	0.00	0.20	0.19	0.15	0.38	0.00	0.22	0.28	0.00	0.18
Cl	0.13	0.07	0.00	0.05	0.08	0.12	0.10	0.00	0.05	0.05	0.00	0.04
OH	3.75	3.69	4.04	4.06	3.66	3.69	3.48	4.13	4.06	3.64	4.20	3.99
Σ	4.03	3.95	4.04	4.30	3.94	3.96	3.95	4.13	4.33	3.96	4.20	4.20
Sum Cat#	19.41	19.39	19.35	20.00	19.36	19.43	19.35	19.41	19.91	19.37	19.41	19.56
XMg	0.47	0.46	0.47	0.49	0.31	0.33	0.28	0.31	0.30	0.23	0.25	0.21
XFe	0.53	0.54	0.53	0.51	0.69	0.67	0.72	0.69	0.70	0.77	0.75	0.79
ΣAl(apfu)	2.65	2.94	2.69	2.72	3.07	3.26	3.20	3.39	3.27	3.22	3.36	3.26
Σ Oct	5.54	5.61	5.62	5.56	5.52	5.59	5.54	5.63	5.45	5.52	5.52	5.16
Σ Int	1.84	1.84	1.70	2.14	1.90	1.88	1.86	1.65	2.13	1.89	1.69	2.20
A/CNK	1.45	1.61	1.58	1.26	1.62	1.74	1.73	2.05	1.51	1.71	1.98	1.47
Log (X_{Cl}/X_{OH})	-1.47	-1.73	ND	-1.93	-1.64	-1.49	-1.56	ND	-1.89	-1.90	ND	-2.04
Log (X_{Mg}/X_{Fe})	-0.05	-0.07	-0.05	-0.01	-0.35	-0.32	-0.42	-0.34	-0.37	-0.52	-0.47	-0.59
Log (XF/XOH)	-1.40	-1.30	ND	-1.31	-1.28	-1.40	-0.97	ND	-1.27	-1.12	ND	-1.34
Log (XF/XCl)	0.07	0.44	ND	0.61	0.37	0.10	0.59	ND	0.62	0.78	ND	0.69
X Cl	0.03	0.02	0.00	0.01	0.02	0.03	0.02	0.00	0.01	0.01	0.00	0.01
X F	0.04	0.05	0.00	0.05	0.05	0.04	0.09	0.00	0.05	0.07	0.00	0.04
X OH	0.93	0.94	1.00	0.94	0.93	0.93	0.88	1.00	0.94	0.92	1.00	0.95

Total Al and Fe/(Fe + Mg) variables are commonly used to illustrate compositional relationships of trioctahedral micas from igneous rock suites (Speer 1984). Figure 2 shows the composition of biotite from different units plotted in the annite – siderophyllite – phlogopite – eastonite quadrilateral (ASPE). They show variation in composition in a way that biotites from granodiorite and monzogranite units are fairly Fe rich whereas those from quartzdiorites are relatively Mg rich (Fig. 2). Biotite from granodioritic rocks of BGC exhibits a fairly wide range of Al values reaching up to 3.32 apfu, at very narrow Fe/(Fe + Mg) ratios (0.66 to 0.75). The biotite samples from the monzogranite like granodiorite define a field with a relatively narrow range but slightly higher Fe/(Fe + Mg) with total Al values range from 3.16 to 3.33 apfu (Fig. 2). Biotite from the quartzdiorite shows approximately a fixed range of Fe/(Fe + Mg) and a large variation of moderate Al contents (2.54 to 3.04 apfu) in the ASPE quadrilateral (Fig. 2). Their lower Fe/(Fe + Mg) ratios indicate that biotite from quartzdiorite is enriched in Mg and contains less A1 with respect to the other units.

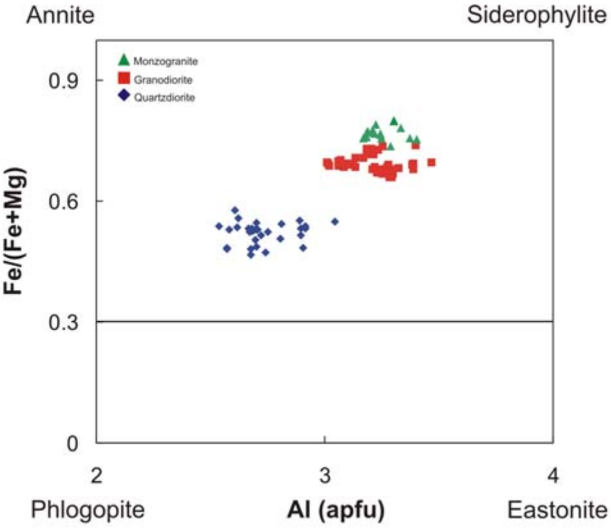

Figure 2: composition of biotite from different units of BGC plotted in the annite – siderophyllite – phlogopite – eastonite quadrilateral (ASPE). Note that biotite from quartzdiorites plots separately from those of granodiorites and monzogranites.

The halogen contents of biotite from the middle Jurassic plutonic rocks of BGC are shown in Table 2. Biotite grains in granodiorite and monzogranite of BGC have relatively higher F contents than those in the quartzdiorites. Biotites from quartzdiorites, granodiorites and monzogranites contain 0.07–0.62, 0.06-0.98 and 0.21-0.86 wt% fluorine with average of 0.24, 0.44 and 0.55 wt% respectively (Table 2). Chlorine contents in biotite from monzogranites are 0.11 to 0.22 wt% (on average 0.17 wt%) and 0.01 to 0.6 wt% in granodiorites (on average 0.37 wt%) which are lower than those of 0.22 to 0.52 wt% in quartzdiorites (on average of 0.41 wt%) (Table 2).

Crystallization conditions of biotite

The composition of biotites depends on a number of interdependent variables e.g. P, T, fO_2, fH_2O, and element activities, one of which must be defined either empirically or indirectly so as to determine the others.

Estimation of oxygen fugacity and redox condition

In the Fe^{2+}-Fe^{3+}-Mg ternary diagram (Wones & Eugster, 1965), the comparison of biotite compositions with common oxygen buffers (quartz—fayalite—magnetite QFM, nickel—nickel oxide, NNO and hematite—magnetite, HM) shows all biotite samples from different units of BGC plotted above the NNO buffer (Fig. 3). Our results indicate relatively more oxidizing conditions for quartzdiorite and granodiorite and slightly reducing conditions for monzogranite but still above NNO buffer. The oxidizing conditions of the quartzdiorite magma are also supported by the presence of titanomagnetite and euhedral titanite (Ishihara, 1977; Wones, 1989). Imposed on the Figure 3 is the discrimination boundary of Buda *et al.*, (2004), the boundary between magnetite and ilmenite granitoids. As it can be seen, biotite compositions from monzogranite fall below this line, in the field of ilmenite granitoids, while those from granodiorite and quartzdiorite plot in the field of magnetite granitoids. This is consistent with the presence of magnetite, allanite and euhedral titanite in the latter rocks.

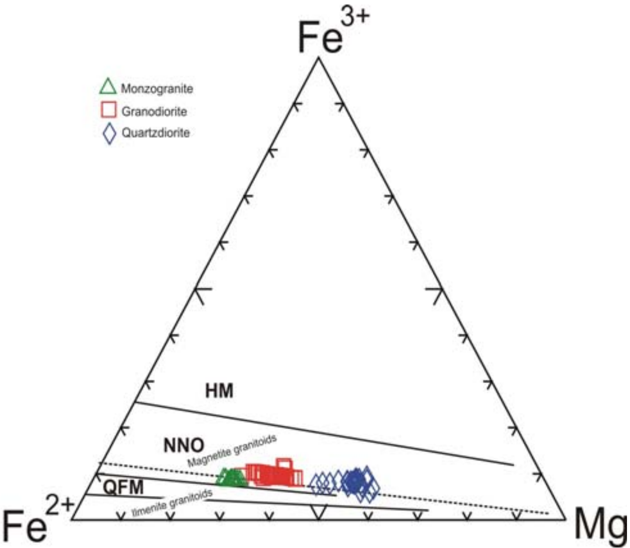

Figure 3: Composition of biotite from BGC plotted in the Fe^{2+}-Fe^{3+}-Mg ternary diagram (Wones & Eugster, 1965), along with the three common oxygen fugacity buffers: quartz – fayalite – magnetite (QFM), nickel–nickel oxide (NNO), and hematite–magnetite (HM). The solid line separates magnetite granites realm from ilmenite granites one.

Quantitative determination of Oxygen and water fugacity

Granitoid biotites react to form a number of assemblages, among them biotite-K-feldspar-magnetite act as a buffer of oxygen and water fugacities in the magma (Wones & Eugster 1965). Estimating the $fO2$ in the magma and activities of magnetite and K-feldspar and the activity of annite in biotite with some certainty result in deriving the water fugacity through the reaction (Wones 1972; Czamanske and Wones 1973):

$\log f\ H_2O = 7409/T + 4.25 + 0.5\log f\ O_2 + \log a_{ann} - \log aK_f - \log a\text{mag}$

Where T is in °K, and activities are shown rather than molar fractions. The ideal activity model of Mueller (1972), Wones (1972) and Czamanske and Wones (1973) is used here for annite in biotite.

$a_{ann} = (X_{Fe2+})^3$

The activity of K-feldspar is 0.6 for magmatic temperatures (Czamanske & Wones 1973) and activity of most re-equilibrated magnetites is close to 1 (ideal). Oxygen fugacity (Log $f\ O_2$) of –17.66 bars and water fugacity ($f\ H_2O$) of 400 and 700 bars were calculated for granodiorite and monzogranites respectively, whereas the Log fO_2 of -15.4 to -17.5 bars and water fugacity ($f\ H_2O$) of 200 to 560 bars were calculated for quartzdiorite (Table 3).

Table 3: Calculated oxygen and water fugacity from biotites equilibration pressure and temperature based on calibration of Wones, 1972; Czamanske and Wones, 1973; a_{ann} calculated after Mueller (1972) and Wones (1972); Annite activity after Czamanske and Wones (1973); pressure and temperature after Ahmadi-Khalaji *et al.,* (2007).

	Quartzdiorite	***Granodiorite***	***Monzogranite***
Average X_{Fe}^{2+}	0.36	0.46	0.52
Activity of Kf	0.60	0.60	0.60
Activity of magnetite	1.00	1.00	1.00
Temperature	732-653 ºC	649.00 ºC	649.00 ºC
Pressure	0.43-1.61 kbar	1 kbar	1 kbar
log fH_2O = 7409/T+4.25+0.5log fO2+log a(ann) - log aKf - log a(mag)	2.79 2.36	2.67	2.83
fH_2O	562.00 200.00	398.00	707.00
log $fO2$ = -24930/T+9.36+0.046(P-1)/T	-15.44 -17.55	-17.67	-17.67

Discussion:

Petrogenetic implication

Biotite composition may be a reliable indicator of the origin of the parental magma (Burkhard, 1993; Lalonde & Bernard, 1993; Aydin *et al.,* 2003; Machev *et al.,* 2004). High Mg and low Al^{VI} contents of biotite from the quartzdiorite reflect a slightly fractionated magma (Hecht, 1994). This is typical of the I-type granitoids, where a contribution of mantle material to melt and mixing process is assumed.

The biotite in granodiorite and monzogranite from the Boroujerd complex reflects almost identical features. The higher Al^{VI} content in biotite compared to the quartzdiorite biotites is supposed to crystallize from a relatively Al-rich magma. The geochemical and isotopic data on BGC provided by Ahmadi-Khalaji *et al.,* (2007) indicate that these rocks originated by partial melting of crustal protoliths as a result of emplacing of mantle melts into the lower crust, providing heat for crustal anatexis.

Below, we compare the compositional fields or trends of biotite from Boroujerd granitoids with those of well-documented granitic suites from other belts e.g. Canadian Appalachian granites (Shabani *et al.,* 2003) and California batholiths (Ague & Brimhall, 1988) to shed light on the petrogenetic and tectonomagmatic characteristics of their host rocks. In general, compositions of biotite from the Boroujerd granitoid complex of SSZ show a range of Fe/(Fe + Mg) values that is nearly identical to that defined by continental arc suites such as the Coastal batholith of Peru (Mason 1985), the Bishop suite of the Wopmay orogen (Lalonde & Bernard 1993), and the magnetite-series granites of Japan (Czamanske *et al.,* 1981), but with greater variations in total Al contents, suggesting a greater contribution from metasedimentary material to their magmas.

Biotite compositions from the granodioritic and monzogranitic units shown in Figure 2 are characterized by moderate to relatively high total Al contents. Those from the quartzdiorite show a trend defined by approximately constant Fe/(Fe + Mg) values and lower total Al values with respect to other units. Biotite from quartzdiorite is more enriched in MgO hence lower FeOtot/MgO. As it was shown above, biotite from both granodiorites, and monzogranites in Boroujerd complex are defined each by a nearly horizontal trend of increasing total Al at relatively constant Fe/(Fe + Mg) in the ASPE quadrilateral (Fig. 2). This kind of trend has been frequently reported in the literature, e.g., in the I–SCR (strongly contaminated and reduced I-type) granites of the California batholiths (Ague & Brimhall, 1988), the Hepburn intrusive suite of Wopmay orogen (Lalonde & Bernard 1993) and granitic plutons of Gander zone in New

Brunswick from the Canadian Appalachian orogen (Shabani *et al.*, 2003).

Furthermore log(XF/XOH) versus log(XMg/XFe) diagram of Ague and Brimhall (1988) (Fig. 5) is utilized here in order to evaluate qualitatively the degree of contamination in different units of the Boroujerd complex. The term contamination is used here in a broad sense to refer to interaction of mafic I-type magmas derived from the upper mantle, deep crust or subducted slab with continental crust source component, which may have spatially variable characteristics, by such process as partial melting, magma mixing and assimilation. Variables of this plot reflect the ƒO2 and ƒHF/ƒH2O conditions of biotite crystallization. In addition, in the biotite structure F and OH are the primary substitutional anions in the hydroxyl sites, whereas Mg and Fe are the predominant element in octahedral sites. In accordance with Ague and Brimhall (1988) rocks containing biotites with log(XMg/ XFe)> -0.21 are divided into three subgroups based upon increasing F/OH: I-WC, I-MC and I-SC (weakly, moderately and strongly contaminated I-type, respectively). Log(XMg/ XFe) ranges from -0.452 to 0.074 in the analyzed biotites and most of samples from qaurtzdioritic unit in Boroujerd complex fall within I-MC field whereas the other two units, containing biotites with log(XMg/ XFe)< -0.21, classified as I-SCR type (strongly contaminated reduced I-type) (Fig. 4). These evidences are in agreement with calculated oxygen fugacity and Al contents (peraluminousity) of BGC biotites.

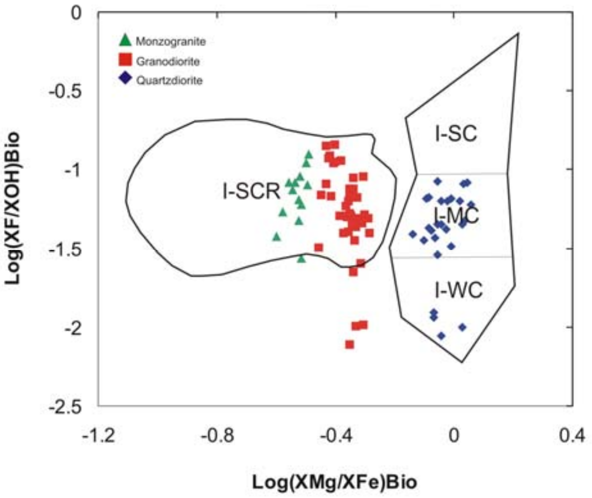

Figure 4: Composition of biotites from different units of BGC in the log(XF/XOH) versus log(XMg/XFe) plot of Ague and Brimhall (1988). I-WC: Weakly contaminated I-type; I-MC and I-SC: Moderately and strongly contaminated I-type; I-SCR: Strongly contaminated and reduced I-type.

Tectonomagmatic implication:

Abdel-Rahman (1994) collected a large number of biotite analyses from literature and made-up different diagrams discriminating biotites from anorogenic extension-related peralkaline granites, calc-alkaline I-type orogenic suites and peraluminous rocks including S-type granites. These diagrams are capable to discriminate the composition of biotite from different tectonic settings in terms of its FeO, MgO, and Al2O3 contents. Among those, ternary FeO*–MgO–Al2O3 plot is employed (Fig. 5), which reflects variations in redox state and peraluminosity much like the ASPE quadrilateral.

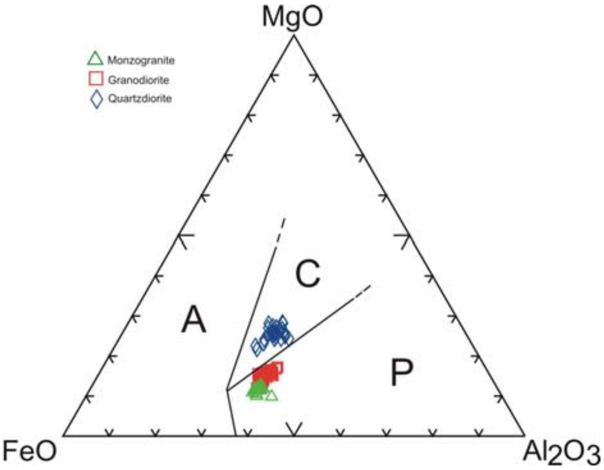

Figure 5: Composition of biotite from BGC plotted in the discrimination diagrams of Abdel Rahman, (1994). A: alkaline, C: calc-alkaline, and P: peraluminous granite fields. FeO* = [FeO + (0.89981*Fe_2O_3)].

In the FeO*–MgO–Al2O3 diagram of Abdel-Rahman (1994), biotite compositions from the Boroujerd complex in SSZ are distributed between the calc-alkaline and peraluminous fields (Fig. 5); compositions of biotite from the qaurtzdioritic rocks fall principally in the C (calc-alkaline) field, whereas those from the peraluminous granites e.g. granodioritic and monzogranitic unit, plot almost exclusively in the P (peraluminous) field. The composition of biotite from qaurtzdioritic unit principally falls in the calc-alkaline subduction related I-type field (Fig. 5) which is consistent with their tectonomagmatic characteristics investigated by Ahmadi-Khalaji *et al.*, (2007) on the basis of whole rock geochemistry. However, granodioritic and monzogranitic units including metaluminous to slightly peraluminous I-type, and some peraluminous S-type granites whose major- and trace-element compositions are comparable to those of granite suites from classical volcanic arc granites, convergent and collisional environments, respectively.

Conclusions:

Granites from different units of Boroujerd complex in SSZ are interpreted as having formed within a subduction-related environment. They contain biotite that is compositionally possessing moderate to relatively high Al contents, suggestive of significant contributions from either aluminous metasedimentary material or magmas originated from aluminous supracrustal material.

Biotite compositions from metaluminous I-type quartzdioritic units have slightly lower content of Al_2O_3 in contrast to the other two units, but being moderately enriched in Mg, they plot in the calc-alkaline I-type field in the tectonic discrimination diagram. These compositional features of biotite are consistent with the nature of their host rocks.

The granodiorite and monzogranite plutons are peraluminous and belong to the I-type granites of Chappell and White (1974). Biotite compositions from these units considered to be derived entirely from crustal material, showing a remarkable increase in both total Al and Fe.

References

Abdel-Rahman, A. M., 1994. Nature of biotites from alkaline, calc-alkaline and peraluminous magmas. Journal of Petrology 35: 525-541

Ague, J.J., Brimhall G. H., 1988. Regional variations in bulk chemistry, mineralogy and the compositions of mafic and accessory minerals in the batholiths of California. Geological Society of America Bulletin, 100: 891-911

Ahmadi-Khalaji, A., Esmaeily, D., Valizadeh, M.V., Rahimpour-Bonab, H., 2007. Petrology and geochemistry of the granitoid complex of Boroujerd, Sanandaj- Sirjan Zone, Western Iran. Journal of Asian Earth sciences, 29: 859-877.

Ahmadi-Khalaji, A., Tahmasbi Z., Zarei Sahamieh R., 2009. Petrography and mineral chemistry of Boroujerd pluton (Sanandaj-Sirjan zone, western Iran). Journal of Applied Sciences 9(5): 843-853

Aydin, F., Karsli ., Sadiklar M., 2003. Mineralogy and Chemistry of Biotites from Eastern Pontide Granitoid Rocks, NE-Turkey: Some Petrological Implications for Granitoid Magmas**.** Chemie der Erde, 63: 163-182.

Best, M. G., Mercy E. L. P., 1967. Composition and crystallization of mafic minerals in the Guadelupe igneous complex, California. American Mineralogist 52, 436-474.

Bónová, K., Broska I., Lipka J., Tóth I., 2006. Composition of biotites from Cierna Hora granitoids (Western Carpathians) as an indicator of the granite tectonic setting. Geolines, vol. 20

Bónová, K., Broska I. and Igor P., 2010. Biotite from Ciernahora Mountains granitoids (Western Carpathians, Slovakia) and estimation of water contents in granitoid melts. Geologica Carpathica, 1335-0552

Buda, G., Koller F., Kovács J. Jaromír, Ulrych J., 2004. Compositional variation of biotite from Variscan granitoids in Central Europe: A statistical evaluation. Acta Mineralogica-Petrographica, Szeged, 45(1): 21-37

Burkhard D.J.M., 1991. Temperature and redox path of biotite-bearing intrusives: a method of estimation applied to S- and I-type granites from Australia. Earth and Planetary Science Letter 104: 89-98.

Burkhard D. J. M., 1993. Biotite crystallization temperatures and redox states in granitic rocks as indicator for tectonic setting. Geol. Mijnbouw 71: 337-349

Chappell B. W. and White A. J. R., 1974. Two contrasting granite types. Pacific Geology, 8: 173-4

Czamanske G. K. and Wones D. R., 1973. Oxidation during magmatic differentiation, Finnmarka complex, Oslo area, Norway 2. The mafic silicates. Journal of Petrology, 14: 349-380.

Hecht L., 1994. The chemical composition of biotite as an indicator of magmatic fractionation and metasomatism in Sn-specialised granites of the Fichtelgebirge (NW Bohemian massif, Germany). In: R. Seltmann, H. Kämpf and P. Möller (Eds), Metallogeny of collisional orogens. Czech Geological Survey, Prague, 295-300

Ishihara S., 1977. The magnetite-series and ilmenite-series granitic rocks. Mining Geology, 27: 293-305

Lalonde A. and Bernard P., 1993. Composition and color of biotite from granites: Two useful properties in the characterization of plutonic suites from the Hepburn internal zone of Wopmay orogen, NW Territories. Canadian Mineralogist, 31: 203-217

Li, z., Tainosho Y, Shiraishi K. and Owada M, 2003. Chemical characteristics of fluorine-bearing biotite of early Paleozoic plutonic rocks from the Sør Rondane Mountains, East Antarctica, Geochemical Journal, 37: 145-161

Machev P., Klain L. and Hecht L., 2004. Mineralogy and chemistry of biotites from the Belogradchik pluton – some petrological implications for granitoid magmatism in North-West Bulgaria. Bulgarian Geological Society, Annual Science Conference "Geology 2004", 16-17. 12. 2004, 48-50.

Mahmoudi S., Corfu F., Masoudi F., Mehrabi B., Mohajjel M., 2011. U–Pb dating and emplacement history of granitoid plutons in the northern Sanandaj–Sirjan Zone, Iran. Journal of Asian Earth Sciences, 41: 238-249

Mason, G.H., 1985. The mineralogy and textures of the Coastal batholith, Peru. In: W.S. Pitcher et al., (Eds.). Magmatism at a Plate Edge, the Peruvian Andes Wiley, New York, N.Y. 156-166.

Moazami Goudarzi F., 2006. Application of biotite in the petrogenetic study of Boroujerd granitoids, Kharazmi University, M.Sc thesis (In Persian)

Mueller R., 1972. On the stability of biotite. American Mineralogist, 57: 300-316.

Nachit H., Razafimahefa N., Stussi J.M. and Carron J. P., 1985. Composition chimiques des biotite et typologie magmatique des granitoids. C R Acad. Sci, 301: 813 -818

Nachit H., Ibhi A., Abia E. H., Ben Ohod M., 2005. Discrimination between primary magmatic biotites, reequilibrated biotites and neoformed biotites. Geosciences, 337, 1415-1420.

Patino-Douce, A.E., 1993. Titanium substitution in biotite: an empirical model with applications to thermometry, O2 and H2O barometries, and consequences for biotite stability. Chemical Geology, 108: 133-162.

Patino-Douce, A.E., Johnston, A.D. and Rice, J.M., 1993. Octahedral excess mixing properties in biotite: a working model with applications to geobarometry and geothermometry. American Mineralogist, (78): 113-131.

Pouchou JL, Pichoir F., 1984. A new model for quantitative analysis. I. Application to the analysis of homogeneous samples. La Récherche Aerosp, 3: 13-38

Pouchou JL, Pichoir F., 1985, "PAP" (Z) procedure for improved quantitative microanalysis. - In: Armstrong, J.T. (Eds): Microbeam Anal. 1985, San Francisco Press, San Francisco, California: 104-106"

Shabani A. A. T. Lalonde A. E., Whalen J. B., 2003. Composition of biotite from granitic rocks of the Canadian Appalachian: A potential tectonomagmatic indicator? The Canadian Mineralogist, 41: 1381-1396

Shabani A. A. T. Masoudi F., Tecce F., 2010. An investigation on the composition of biotite from Mashhad granitoids, NE Iranian, Journal of Science, Islamic Republic of Iran 21(4): 321-331.

Speer, J.A., 1984. Micas in igneous rocks. In: Micas. Bailey S.W., (Eds.). Review of Mineralogy, 13: 299-356.

Stone M., Klominsky J., and Rajpoot G. S., 1997. Composition of trioctahedral micas in the Karlovy Vary pluton, Czech Republic and a comparison with those in the Cornubian Batholith, SW England. Mineralogical Magazine, 61(6): 791-807

Stone M., 2000. Petrogenetic implications from biotite compositional variations in the Cornubian granite batholith. Mineralogical Magazine, 64(4): 729-735

Wones, D.R. and Eugester, H.P., 1965, Stability of biotite: experiment, theory, and application. American Mineralogist, 50: 1228-1272.

Wones D. R., 1989. Significance of the assemblage titanite + magnetite + quartz in granitic rocks. American Mineralogist, 74: 744-749

Wones, D. R., 1972. Stability of biotite: a reply. American Mineralogist, 57: 316-317.